

# Thermal Expansion of $\text{Pb}_2\text{Sr}_2\text{Y}_{1-x}\text{Ca}_x\text{Cu}_3\text{O}_{8+\delta}$

H. M. O'Bryan\* and P. K. Gallagher

AT&T Bell Laboratories, Murray Hill, New Jersey 07974

Received May 2, 1989

The thermal expansion of  $\text{Pb}_2\text{Sr}_2\text{Y}_{1-x}\text{Ca}_x\text{Cu}_3\text{O}_{8+\delta}$  has been measured between 25 and 700 °C for  $x = 0, 0.2, \text{ and } 0.4$ . Measurements were made on ceramic samples with  $\delta = 0$  during heating at 4 °C/min in  $\text{N}_2$  and  $\text{O}_2$  atmospheres. In  $\text{N}_2$  the coefficient of thermal expansion is  $\sim 13 \text{ ppm}/^\circ\text{C}$  for all compositions. In  $\text{O}_2$  the expansion varies greatly with temperature as the samples undergo both oxidation and reduction. The expansion mimics previously reported gravimetric data. Two maxima of  $\sim 1.4\%$  are found near 550 and 700 °C. The lattice expansion on oxidation contrasts to the shrinkage observed when  $\text{Ba}_2\text{YCu}_3\text{O}_{8.2}$  is oxidized.

## Introduction

A family of high- $T_c$  oxide superconductors that have the general formula  $\text{Pb}_2\text{Sr}_2\text{Ln}_{1-x}\text{M}_x\text{Cu}_3\text{O}_{8+\delta}$  has been reported by Cava et al.<sup>1</sup> and Subramanian et al.<sup>2</sup> In this formula  $\text{Ln} = \text{La, Y, or a rare-earth metal}$  and  $\text{M} = \text{Ca or Sr}$ . The structural basis for this family is double planes of corner-shared  $\text{CuO}_5$  pyramids that are separated by planes containing the eight-coordinated  $\text{Ln}$  atoms. Figure 1 shows the structure with Ca as the M atom.<sup>1</sup> The arrangement of double-pyramidal planes ( $\text{PbO}_5\text{--CuO}_5\text{--PbO}_5$ ) is unique to this family. It has been proposed that when  $x$  and  $\delta = 0$ , the Cu atoms in the sheet between the  $\text{PbO}_5$  layers are monovalent while those in the corner-shared pyramids are divalent. Substitution of  $\text{M}^{2+}$  for  $\text{Ln}^{3+}$  increases the valence of the pyramidal Cu atoms at constant oxygen content ( $\delta$ ). The addition of oxygen ( $\delta > 0$ ), which locates itself between the  $\text{PbO}_5$  layers, increases the valence of the Cu atoms in the central sheet. The extent to which this oxidation also affects the pyramidal Cu is uncertain, but some effect is expected.

The oxidation-reduction behavior of  $\text{Pb}_2\text{Sr}_2\text{Y}_{1-x}\text{Ca}_x\text{Cu}_3\text{O}_8$  has recently been examined in detail by using thermogravimetric (TG) and X-ray diffraction (XRD) techniques.<sup>3</sup> In oxidizing atmospheres, increasing temperature produces oxidation up to 500 °C, reduction between 600 and 650 °C, and oxidative decomposition above 650 °C. As the amount of oxygen absorbed changes, the orthorhombic structure was observed to transform to tetragonal, then revert to orthorhombic, and eventually decompose. XRD data indicated that the lattice dimensions increase with oxidation. The present study examines the thermal expansion during heating in oxygen and nitrogen for ceramic samples with  $x = 0.0, 0.2, \text{ and } 0.4$ . A comparison is also made with the behavior of  $\text{Ba}_2\text{YCu}_3\text{O}_{7-x}$  treated under similar conditions.

## Experimental Procedures

Compositions of  $\text{Pb}_2\text{Sr}_2\text{Y}_{1-x}\text{Ca}_x\text{Cu}_3\text{O}_8$  with  $x = 0.0, 0.2, \text{ and } 0.4$  were prepared as described by Cava.<sup>1</sup> A precursor was made by reacting the proper amounts of  $\text{SrCO}_3$ ,  $\text{CaCO}_3$ ,  $\text{Y}_2\text{O}_3$ , and  $\text{CuO}$  at 920 °C for 16 h in air. After addition of  $\text{PbO}$ , the mixture was reheated at 920 °C for 1 h. The resulting powder was formed into 6-mm-diameter pellets, sintered at 850 °C for 24 h in 1% oxygen, and quenched. Prior to use in the dilatometer each ceramic pellet was heated to 750 °C for 8 h in nitrogen and cooled in nitrogen. Initial density and the X-ray structure were determined after various heatings.

The thermal expansion in either nitrogen or oxygen was measured with a Theta Research dilatometer at a heating rate of 4 °C/min. Isothermal data were obtained while changing the atmosphere. It was not possible to obtain expansion data above 720 °C because of reaction between the sample and fused silica holder in the dilatometer. Attempts to isolate the sample with 0.001-in. Au foil were not successful because of reaction, presumably Pb diffusing through the Au to attack the silica.

## Results and Discussion

XRD results for samples quenched after 24 h at 865 °C in 1% oxygen showed that only the  $x = 0.0$  composition remained single phase. The amount of second phase, referred to previously as pseudocubic,<sup>3</sup> increased as the Ca content  $x$  increased. After treatment in  $\text{N}_2$  at 750 °C for 8 h, all compositions were single-phase orthorhombic. Table I lists the ceramic densities obtained by geometric measurements and the lattice constants obtained from the powder XRD. The calculated X-ray density for  $x = 0.25$  is  $7.1 \text{ g}/\text{cm}^3$ .<sup>2</sup>

In nitrogen (Figure 2) all compositions showed uneventful expansions with similar coefficients of thermal expansion (CTE) near  $13 \text{ ppm}/^\circ\text{C}$  for 25–400 °C. These are consistent with the small changes in oxygen content in inert atmospheres.<sup>3</sup> In oxygen each composition showed a complicated expansion profile that consisted of two maxima and one minimum (Figure 3). For  $x = 0$  the initial maximum occurs near 550 °C and  $\Delta l/l = 11 \times 10^{-3}$  while the second occurs at 720 °C with a larger  $\Delta l/l$  of  $16 \times 10^{-3}$ . A minimum is found at 620 °C having  $\Delta l/l = 8 \times 10^{-3}$ . With increasing  $x$  the first maximum becomes larger and shifts to higher temperature, while the second maximum decreases in both height and temperature. The minimum remains near 630 °C for all compositions, but the sample having  $x = 0.4$  shows the least shrinkage. Table I lists the coefficients of thermal expansion in nitrogen as well as the maximum and minimum expansions in oxygen.

In Figure 4,  $\Delta l/l$  and TG data, with the weight value converted into oxygen content,  $\delta$ , are shown for the  $x = 0$  ceramic. Included in this figure are the phases determined in ref 3 for samples quenched after heating in oxygen. The first region of oxygen pickup (325–525 °C) corresponds to the first region of rapid expansion. The displacement of the temperature for the  $\Delta l/l$  maximum relative to the  $\delta$  maximum is only apparent. It results from the superposition of the thermal and oxidative expansions. When these are considered separately, 525 °C becomes the temperature at which both maxima occur. The expansion minimum and second maximum are similarly matched to variations in oxygen content. As previously noted the orthorhombic and tetragonal structures occur below 630 °C while decomposition to a pseudocubic phase occurs above that temperature. Interestingly, the minimum in

(1) Cava, R. J.; et al. *Nature* 1988, 336, 211.

(2) Subramanian, M. A.; et al. *Physica C* 1989, 157, 124.

(3) Gallagher, P. K.; et al. *Chem. Mater.* 1989, 1, 277.

(4) Gallagher, P. K.; O'Bryan, H. M.; Sunshine, S. A.; Murphy, D. W. *Mater. Res. Bull.* 1987, 22, 995.

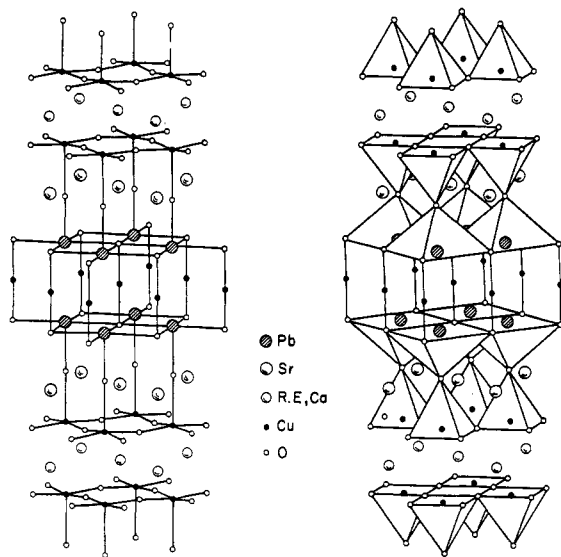


**Figure 1.** Crystal structure for  $\text{Pb}_2\text{Sr}_2\text{YCu}_3\text{O}_8$ : (left) bonding scheme for O-Pb and O-Cu bonds; (right) arrangement of Cu-O and Pb-O polyhedra.<sup>1</sup>

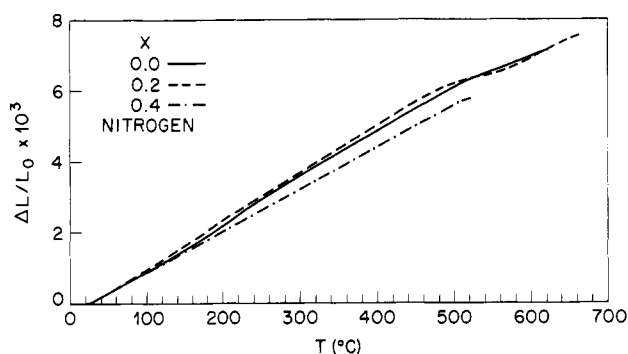


**Figure 2.** Thermal expansion of  $\text{Pb}_2\text{Sr}_2\text{Y}_{1-x}\text{Ca}_x\text{Cu}_3\text{O}_8$  in nitrogen for  $x = 0, 0.2$ , and  $0.4$ ; heating rate  $4^\circ\text{C}/\text{min}$ .

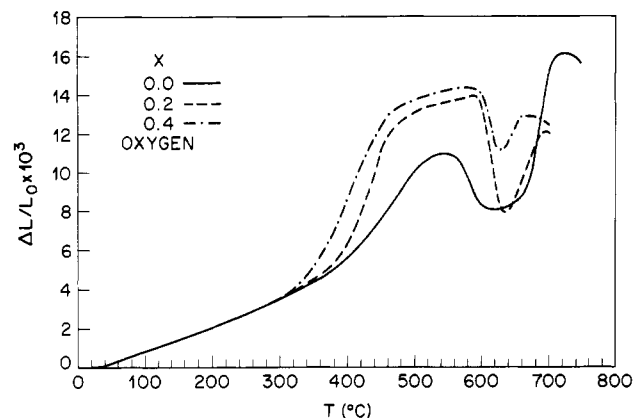


**Figure 3.** Thermal expansion of  $\text{Pb}_2\text{Sr}_2\text{Y}_{1-x}\text{Ca}_x\text{Cu}_3\text{O}_8$  in oxygen for  $x = 0, 0.2$ , and  $0.4$ ; heating rate  $4^\circ\text{C}/\text{min}$ .

expansion that corresponds to  $\delta \approx 0$  falls on the extrapolation of the low-temperature expansion. The CTE for the extrapolated expansion is  $\sim 14 \text{ ppm}/^\circ\text{C}$ , which is quite similar to the value found for the  $\text{N}_2$  data in Figure 2. The differences in expansion shown in Figure 3 for the various values of  $x$  (Ca contents) can thus be understood in terms of the ease of oxidation. The ceramic with  $x = 0.4$  has been shown to oxidize most easily.<sup>3</sup> Thus it begins its rapid expansion at the lowest temperature.

The lattice parameters obtained by powder XRD for quenched samples having various values of  $\delta$  in the orthorhombic/tetragonal region have been used to calculate

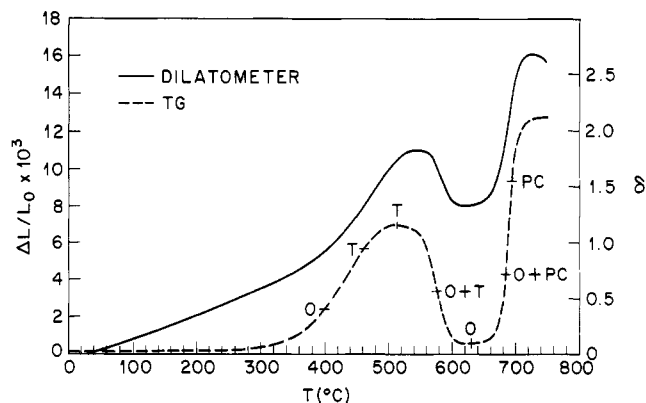


**Figure 4.** Thermal expansion and TG curves for  $\text{Pb}_2\text{Sr}_2\text{YCu}_3\text{O}_8$  in oxygen; heating rate  $4^\circ\text{C}/\text{min}$ .

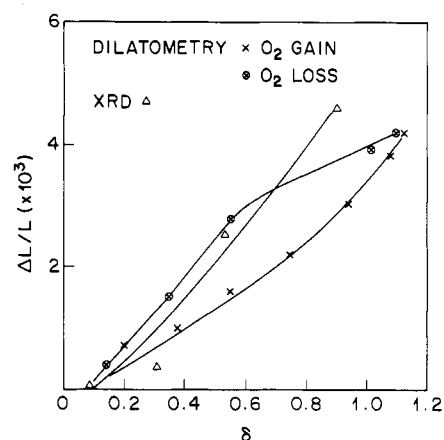


**Figure 5.** Expansion vs  $\delta$  for  $\text{Pb}_2\text{Sr}_2\text{YCu}_3\text{O}_{8+\delta}$  (dilatometric data corrected for thermal expansion).

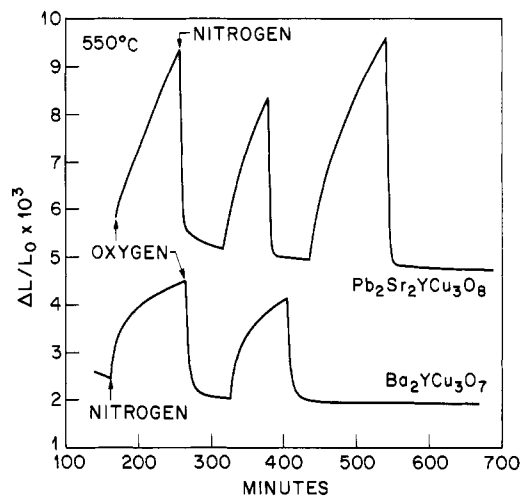


**Figure 6.** Expansion vs time for  $\text{Ba}_2\text{YCu}_3\text{O}_7$  and  $\text{Pb}_2\text{Sr}_2\text{YCu}_3\text{O}_8$  as the atmosphere is switched between nitrogen and oxygen at  $550^\circ\text{C}$ .

lattice volumes. The differences in lattice volume have been used to calculate average  $\Delta l/l$ 's, and these  $\Delta l/l$ 's are compared to those measured by dilatometry in Figure 5. The quenched samples were heated at  $2^\circ\text{C}/\text{m}$ , while the dilatometric data have been distinguished according to whether they were obtained from the oxygen-gain or oxygen-loss regions of Figure 4. Better agreement is found between the XRD and oxygen-loss data. Since the oxygen-loss data were obtained at higher temperatures, these values are closer to the equilibrium expansions. The

Table I

|  | Ca content (x)   |                    |   |
|--|------------------|--------------------|---|
|  | 0.0              | 0.2                | 0.4   |
| phases present after quenching from 865 °C/1% O <sub>2</sub> | orthorhombic (O) | O + sl pseudocubic | O + major pseudocubic + minor SrPb O <sub>3</sub> |
| phases present after quench from 750 °C/N <sub>2</sub>       | O                | O                  | O   |
| lattice parameters   |                  |                    |   |
| a, Å   | 5.38             | 5.38               | 5.37  |
| b, Å   | 5.42             | 5.42               | 5.41  |
| c, Å   | 15.70            | 15.73              | 15.70   |
| density, g/cm <sup>3</sup>                                   | 4.3              | 4.4                | 4.8   |
| CTE in ppm °C <sup>-1</sup> in M <sub>2</sub> at 25–400 °C   | 13.7             | 13.5               | 12.9  |
| CTE in ppm °C <sup>-1</sup> in O <sub>2</sub> at 25–250 °C   | 13.6             | 14.4               | 13.3  |
| T for max, °C  | 550              | 591                | 582   |
| Δl/l × 10 <sup>3</sup> at max                                | 12.1             | 13.9               | 14.3  |
| T at min, °C   | 620              | 640                | 627   |
| Δl/l × 10 <sup>3</sup> at min                                | 8.0              | 7.6                | 11.0  |
| T for max, °C  | 720              | 692                | 670   |
| Δl/l × 10 <sup>3</sup> at max                                | 10.1             | 12.1               | 12.9  |

slower heating rate for the XRD data should also produce expansions that are near to the equilibrium value. Thus the improved agreement is expected.

The change in dimensions with oxidation can also be shown by isothermal dilatometry while the atmosphere is cycled between nitrogen and oxygen. Figure 6 shows that at 550 °C Pb<sub>2</sub>Sr<sub>2</sub>YCu<sub>3</sub>O<sub>8</sub> expands ~0.35% during the first 60 min after oxygen is introduced. When nitrogen is introduced, a similar shrinkage occurs. The kinetics of the Δl/l change are seen to depend strongly on whether the sample is gaining or losing oxygen with oxidation occurring more slowly. Although the change in the dilatometer atmosphere is not instantaneous, the approach to the final oxygen level is quicker when oxygen is introduced since the sample composition has only a very minor effect on the gas composition. When nitrogen is introduced, the gas in the vicinity of the sample remains relatively oxygen-rich as the sample evolves oxygen. Thus the slower kinetics of oxidation are even more remarkable.

Also included on Figure 6 are data for Ba<sub>2</sub>YCu<sub>3</sub>O<sub>6.2</sub> during isothermal dilatometry. The contrast in the effect of oxidation on the lattice dimensions of this compound is striking. The Δl/l shrinkage of ~0.25% which takes place within 60 min accompanies the oxygen gain. In this compound the slower rate of equilibration occurs during reduction in nitrogen. Here the oxygen content of the gas in the vicinity of the sample is increased by evolving oxygen, and the slower kinetics are understandable. It is speculated that the slower oxidation rate of Pb<sub>2</sub>Sr<sub>2</sub>YCu<sub>3</sub>O<sub>8</sub> occurs because the addition of oxygen requires an expansion of the lattice. The expanded lattice at the gas-solid interface is assumed to retard further oxidation in a manner similar to the protective oxide that forms on metals when the specific volume of the oxide is greater than that of the underlying metal.

Another view of the contrast between the oxidative expansions of Ba<sub>2</sub>YCu<sub>3</sub>O<sub>6.2</sub> and Pb<sub>2</sub>Sr<sub>2</sub>YCu<sub>3</sub>O<sub>8</sub> is shown in Figure 7. The former undergoes a continuous shrinkage in the region 400–450 °C as oxygen is incorporated, while above 700 °C the expansion is determined by the smaller coefficient of the tetragonal phase.<sup>5</sup>

Neutron diffraction data are not yet available for Pb<sub>2</sub>Sr<sub>2</sub>YCu<sub>3</sub>O<sub>8+δ</sub>, so bond length changes can only be speculated. It has been proposed that during oxidation the added oxygen takes positions in the central Cu sheet. If this is the case, the competition for the Cu charge permits relaxation of the vertical bonds between these Cu atoms and the oxygen atoms in the PbO<sub>5</sub> planes. Hence

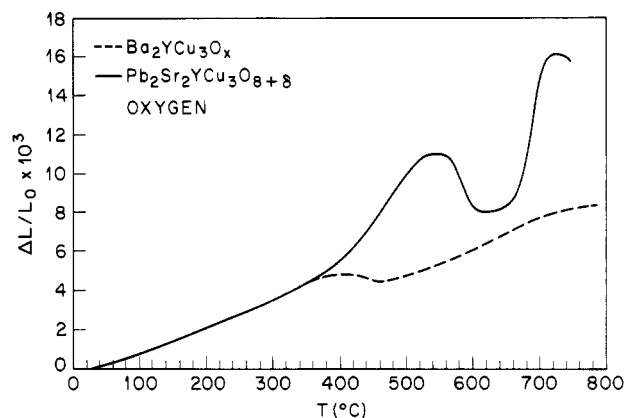


Figure 7. Thermal expansion of Ba<sub>2</sub>YCu<sub>3</sub>O<sub>6.2</sub> and Pb<sub>2</sub>Sr<sub>2</sub>YCu<sub>3</sub>O<sub>8</sub> in oxygen; heating rate 4 °C/min.

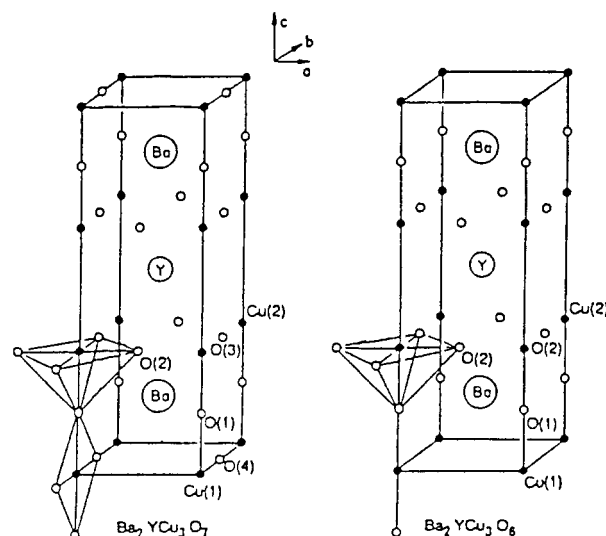


Figure 8. Unit cells for Ba<sub>2</sub>YCu<sub>3</sub>O<sub>7</sub> and Ba<sub>2</sub>YCu<sub>3</sub>O<sub>6</sub> with bonding arrangement.<sup>6</sup>

an expansion along the *c* axis results. A limited effect on the square-pyramidal copper bonding is expected since these bonds are effectively shielded by the Pb atoms. In the case of Ba<sub>2</sub>YCu<sub>3</sub>O<sub>6</sub> (Figure 8) oxidation places oxygen atoms along the *b* axis in the *z* = 0 plane.<sup>6</sup> This results in a change in coordination around the *z* = 0 Cu(1) from

(5) O'Bryan, H. M.; Gallagher, P. K. *J. Mater. Res.* 1988, 3, 619.

(6) Murphy, D. W.; et al. *Chemistry of High Temperature Superconductors*; Nelson, D. L., Whittingham, M. S., George, T. F., Eds.; American Chemical Society: Washington, DC, 1987; p 182.

linear 2-fold to square planar. While the square-pyramidal coordination around the Cu(2) is maintained, there is an effect on the vertical bond length since the affected Cu(1) is directly coupled to Cu(2) by an oxygen atom. A contraction in *c* axis occurs, and the overall sample length shrinks.

When a correlation between Ca content *x* and expansion is sought, it is seen that the location of the Ca in the rare-earth metal plane is too distant to affect directly the O-Cu-O bonding which seems to cause the enormous expansivity changes. A kinetic explanation based on the weight changes previously observed for various Ca contents<sup>3</sup> is suggested. The earlier work showed that for a slower heating rate (1 °C/min) all Ca contents (*x* = 0.0, 0.25, and 0.40) gained similar amounts while faster rates (2 and 5 °C/min) produce lower weight gains for *x* = 0.0. In this study the dilatometric data were obtained at 4 °C/min for all Ca contents. Thus the *x* = 0.0 expansion represents material that has not achieved full oxidation. When Ca is present, more expansion is obtained at the same heating rate. It is therefore suggested that Ca has the effect of facilitating the oxidation process so that oxygen can more quickly enter the lattice and more expansion occurs at the heating rate used.

sion occurs at the heating rate used.

### Conclusions

Oxidation and reduction of  $\text{Pb}_2\text{Sr}_2\text{Y}_{1-x}\text{Ca}_x\text{Cu}_3\text{O}_{8+\delta}$  produce very large changes ( $\sim 5 \times 10^{-3}$ ) in the dimensions of ceramic samples.

Within the orthorhombic/tetragonal phase region these changes are the result of changes in lattice dimensions, particularly the *c* parameter.

At 550 °C the oxidation of  $\text{Pb}_2\text{Sr}_2\text{YCu}_3\text{O}_8$  is much slower than reduction.

The decomposition of the orthorhombic/tetragonal phase to pseudocubic produces an enlarged structure.

The Ca content affects the rate of the oxidative expansion with increasing *x* producing faster oxidation and more expansion at 350–600 °C for a constant heating rate.

Changes in oxygen content produce opposite expansions in  $\text{Ba}_2\text{YCu}_3\text{O}_7$  and  $\text{Pb}_2\text{Sr}_2\text{YCu}_3\text{O}_8$ .

**Acknowledgment.** We are grateful to R. J. Cava for helpful discussions.

**Registry No.**  $\text{Pb}_2\text{Sr}_2\text{Y}_{0.8}\text{Ca}_{0.2}\text{Cu}_3\text{O}_8$ , 122408-19-9;  $\text{Pb}_2\text{Sr}_2\text{Y}_{0.6}\text{Ca}_{0.4}\text{Cu}_3\text{O}_8$ , 122408-20-2;  $\text{Pb}_2\text{Sr}_2\text{YCu}_3\text{O}_8$ , 118557-29-2.

## Particle Size Determination of Cobalt Clusters in Zeolites

Sang Sung Nam,<sup>†</sup> Lennox E. Iton,<sup>‡</sup> Steven L. Suib,<sup>\*,†,§</sup> and Z. Zhang<sup>†</sup>

Department of Chemistry, U-60, University of Connecticut, Storrs, Connecticut 06269-3060, Materials Science Division, Argonne National Lab, Argonne, Illinois 60439, and Department of Chemical Engineering, University of Connecticut, Storrs, Connecticut 06269-3060

Received June 5, 1989

Highly dispersed superparamagnetic cobalt clusters have been prepared in the pores of zeolite Na-X by use of microwave plasma decomposition of  $\text{Co}_2(\text{CO})_8$ . These cobalt clusters have previously been shown to be 100% dispersed and are shown here to be stable to 160 °C. Ferromagnetic resonance data have been simulated to show that the cobalt clusters have a 7-Å-diameter size. Transmission electron microscopy experiments have shown that the cobalt particles are not observable unless sintering at 160 °C occurs. These results are correlated to the catalytic activity of the cobalt clusters in reactions of cyclopropane and hydrogen. The size of the cobalt clusters controls the selectivity of these catalytic reactions.

### Introduction

One of the goals of researchers in the area of catalysis in the past 10 years has been the preparation of highly dispersed materials such as metal clusters.<sup>1</sup> Several approaches have been taken, including solvated metal atom dispersion (SMAD),<sup>2</sup> cluster-derived thermal decompositions,<sup>3</sup> metal atom vaporization,<sup>4</sup> metal vapor reduction,<sup>5</sup> H atom reduction,<sup>6</sup> anchoring,<sup>7</sup> ion implantation,<sup>8</sup> and other methods. When a solid is used to trap the metal clusters, it may be possible to prepare particles smaller than about 15 Å. In this size regime such metal particles may not behave like bulk metals and can give rise to interesting new physical and chemical properties.<sup>9</sup>

Heterogeneous catalytic reactions that depend on the size and shape of metal particles are said to have geometric effects. Electronic effects are due to bonding interactions

between the metal and its support.<sup>10</sup> Electronic effects can be difficult to measure, and there has been consider-

(1) Moskovits, M., Ed. *Metal Clusters*; Wiley Interscience: New York, 1986.

(2) (a) Klabunde, K. J.; Imizu, Y. *J. Am. Chem. Soc.* **1984**, *106*, 2721–2722. (b) Tan, B. J.; Klabunde, K. J.; Tanaka, T.; Kanai, H.; Yoshida, S. *J. Am. Chem. Soc.* **1988**, *110*, 5951–5958. (c) Meier, P. F.; Pennella, F.; Klabunde, K. J. *J. Catal.* **1986**, *101*, 545–548.

(3) (a) Uchiyama, S.; Gates, B. C. *J. Catal.* **1988**, *110*, 388–403. (b) Gates, B. C. In *Catalyst Design, Progress and Perspectives*; Wiley Interscience: New York, 1987; pp 71–139.

(4) (a) Klabunde, K. J. *Chemistry of Free Atoms and Particles*; Academic Press: New York, 1980. (b) Nazar, L. F.; Ozin, G. A.; Hugues, F.; Godber, J.; Rancourt, D. *Angew. Chem., Int. Ed. Engl.* **1983**, *22*, 624–625.

(5) (a) Fraenkel, D.; Gates, B. C. *J. Am. Chem. Soc.* **1980**, *102*, 2478–2480. (b) Lee, J. B. *J. Catal.* **1981**, *68*, 27–33.

(6) Bonneviot, L.; Che, M.; Olivier, D.; Martin, G. A.; Freund, E. *J. Phys. Chem.* **1985**, *90*, 2112–2117.

(7) (a) Jiang, H. J.; Tzou, M. S.; Sachtler, W. M. H. *Appl. Catal.* **1988**, *39*, 255–265. (b) Tzou, M. S.; Teo, B. K.; Sachtler, W. M. H. *Langmuir* **1986**, *2*, 773–776. (c) Tzou, M. S.; Teo, B. K.; Sachtler, W. M. H. *J. Catal.* **1988**, *113*, 220–235.

(8) Haining, I. H. B.; Rabette, P.; Che, M.; Deane, A. M.; Tench, A. *J. Proc. Int. Congr. Catal.*, **7th** **1980**, 317–322.

(9) Romanowski, W. *Highly Dispersed Metals*; Halsted Press: New York, 1987.

<sup>†</sup>Department of Chemistry.

<sup>‡</sup>Materials Science Division.

<sup>§</sup>Department of Chemical Engineering.

\*Author to whom correspondence should be addressed at the Department of Chemistry, University of Connecticut.